Nano World Journal

https://doi.org/10.17756/nwj.2023-s2-064

Research Article | Open Access

Elaboration, Characterization and Structural Study of a Novel Phosphate $(Cd,Co)_5(HPO_4)_2(PO_4)_2.4H_2O$ with the Hureaulite Structure Type

Chaymae El Alami, Jamal Khmiyas*, Mohammed Hadouchi, Abderrazzak Assani, Mohamed Saadi and Lahcen El Ammari

Laboratoire de Chimie Appliquée des Matériaux, Centre des Sciences des Matériaux, Faculty of Science, Mohammed V University in Rabat, Avenue Ibn Battouta, BP 1014, Rabat, Morocco

***Correspondence to:**
Jamal Khmiyas
Laboratoire de Chimie Appliquée des Matériaux,
Centre des Sciences des Matériaux,
Faculty of Science,
Mohammed V University in Rabat,
Avenue Ibn Battouta,
BP 1014, Rabat, Morocco.
E-mail: j.khmiyas@um5r.ac.ma

Received: July 25, 2023
Accepted: September 26, 2023
Published: September 29, 2023

Citation: El Alami C, Khmiyas J, Hadouchi M, Assani A, Saadi M, et al. 2023. Elaboration, Characterization and Structural Study of a Novel Phosphate $(Cd,Co)_5(HPO_4)_2(PO_4)_2.4H_2O$ with the Hureaulite Structure Type. *Nano World J* 9(S2): S378-S382.

Published by United Scientific Group

Abstract

Single crystals of the novel phosphate $(Cd,Co)_5(HPO_4)_2(PO_4)_2.4H_2O$ have been elaborated under mild hydrothermal conditions and analyzed by single-crystal X-ray diffraction. The title compound crystallizes in the Hureaulite-type structure (space group *C2/c*, a = 17.5744(9) Å, b = 9.0723(5) Å, c = 9.4866(5) Å, β = 96.67(3)°, V = 1502.3(1) $Å^3$ and Z = 4). This structure exhibits a cations positional disorder at two sites. The first one is located on the special Wyckoff position 4e(2) and is fully filled by a mixture of $Cd(2)^{2+}/Co(2)^{2+}$ with a respective occupancy ratio of 0.34/0.66. The second one is located on the general position 8f, fully occupied by both $Cd(1)^{2+}/Co(1)^{2+}$. The principal building units are more or less distorted $[(Cd(1)/Co(1))O_5(OH_2)]$, $[(Cd(2)/Co(2))O_6]$, and $[Co(3)O_4(OH_2)_2]$ octahedra with two kinds of regular PO_4 and HPO_4 tetrahedra. This crystal structure results from octahedral pentameric units $M_5^{II}O_{16}(OH_2)_6$ made up of edge-sharing extending parallel to [001] direction. These adjacent entities are interconnected and also linked to each other by the connecting PO_4 and HPO_4 units via common corners so as to build a three-dimensional framework delimiting large holes along the c-axis hosting the water molecules. Bond-valence-sum (BVS) and charge-distribution (CD) methods were applied to validate the suggested structural model.

Keywords

Hureaulite structure, Novel phosphate, X-ray diffraction

Introduction

Nowadays, transition metal-based phosphates are among the most investigated classes of materials. This craze for such phases is supported by their structural richness, their topological diversity and undoubtedly their interesting physical properties [1]. Such assets are directly tied to the particular features of the PO_4, HPO_4 groups and the metallic polyhedra. The organization of such units provides the crystal structures with a high thermal, chemical, and mechanical stability, thus giving rise to suitable interstitial spaces, which can contain cations of different sizes and/or small molecules [2]. In addition, materials comprising hydroxyl $(OH)^-$ and non-zeolitic (H_2O) groups offer a wide range of uses and interesting structural variants. Indeed, hydrated phosphates are essential for the development of supercapacitors [3], steel's surface hardening [4] and the removal of arsenic (As) from water [5]. Furthermore, the combination of transition metals results in outstanding inhibitory, electrochemical, optical, and magnetic characteristics [6]. In line with our hydrothermal investigations of metal orthophosphates, we have already synthesized and analyzed a variety of compounds with various three dimensional frameworks viz. $Mg_7(PO_4)_2(HPO_4)_4$ [7], $Co_2Pb(HPO_4)(PO_4)OH.H_2O$ [8], $M_2Mn_3(HPO_4)_2(PO_4)_2$ (M = Pb [9], Sr [10]), $Ag_2M'_3$(H-

$PO_4)(PO_4)_2$ (M' = Co [11], Ni [12]), $AgMg_3(HPO_4)_2(PO_4)$ [13], $AgSr_4Cu_{4.5}(PO_4)_6$ [14], and $SrFe(HPO_4)(PO_4)$ [15]. The systematic research within CdO-CoO-P_2O_5-H_2O also received significant attention, leading to the novel phosphate $(Cd,Co)_5(HPO_4)_2(PO_4)_2.4H_2O$ that adopts the Hureaulite structure type. The Hureaulite mineral $(Mn,Fe)_5(PO_4)_2(HPO_4)_2.4H_2O$ was initially found by Alluaud [16], described by Dufrénoy [17] and then structurally solved by Moore and Araki [18]. Isotypic phases belonging to this family crystallize in the monoclinic system with the C2/c space group and can be designated by the following general chemical formula: $XY_2Z_2(TO_4)_2(HTO_4)_2{\cdot}4(H_2O)$, where X = Ca, Mn, Cd; Y = Cd, Fe, Ca, Mn; Z = Mn, Fe, Ca, Zn and T = P or As [6]. This paper deals with the hydrothermal elaboration and structural characterization of the new Cd/Co-Hureaulite compound $(Cd,Co)_5(HPO_4)_2(PO_4)_2.4H_2O$.This crystal structure was elucidated by means of single crystal X-ray diffraction and the accuracy of the provided structural model was confirmed using the BVS [19] and CD analysis [20].

Experimentation

Elaboration

This new phase's single crystals were elaborated hydrothermally using a proper reaction mixture of Co, $CdCl_2$, and H_3PO_4 (85% by weight) proportioned in accordance with the molar ratios of Co:Cd:P = 2:1:2. The hydrothermal process was performed under mild conditions at 468 K over 4 days in a suitable autoclave reactor with a 23 ml PTFE lined vessel half filled with deionized water. The reaction product underwent filtering, a distillated water rinse, and room-temperature drying. The obtained purple crystals are consistent with this novel phase. The structure is determined at nanometric scale.

Results and Discussion

Structure determination

An appropriate single crystal was mounted on a Bruker X8 APEXII diffractometer for the X-ray diffraction measurements. The data was gathered using the X-ray Mokα radiation and the φ/ω scan modalities on the full sphere of reciprocal space. The obtained results were then adjusted for Lorentz and polarisation effects using the SAINT program [21]. As a result of further absorption corrections (Multi-scan) performed using SADABS program [22] a total of 10968 intensities, of which 2449 are independent and 2098 meets the I > 2(I) condition were obtained successfully. The structural elucidation of this novel phosphate was carried out using the WinGX suite [23]. This crystal structure was first solved by Direct Methods with the SHELXT 2014/7 program [24] and subsequently refined with the SHELXL2018/3 program [25]. The positioning of Cd, Co, and P atoms was carried out according to structural resolution. The rest of oxygen and hydrogen atoms were introduced to fill the asymmetric unit following multiple iterative refinements and a Fourier-difference analysis. The residual electron densities after the last refinement cycle are $\Delta\rho_{min}$ = -0.81 e.Å^{-3} at 0.88 Å from Co1 and $\Delta\rho_{max}$ = 0.69 e.Å^{-3} at 0.19Å from H6. Crystallographic characteristics, data acquisition details and structural refinement results are given in table 1.

Table 1: Crystal details, X-ray data collection and structure refinement results for $(Cd,Co)_5(HPO_4)_2(PO_4)_2.4H_2O$.

Crystallographic details	
Chemical formula	$(Cd,Co)_5(HPO_4)_2(PO_4)_2.4H_2O$
M_r	846.46
System, space group	Monoclinic, *C2/c*
T (K)	296
a, *b*, *c* (Å)	17.5744 (9), 9.0723 (5), 9.4866 (5)
β (°)	96.671 (3)
V (Å^3)	1502.3 (2)
Z	4
Mo Kα	λ = 0.71073 Å
μ (mm^{-1})	6.52
Data acquisition	
Diffractometer	Bruker X8 *APEX* 2
θ_{min}, θ_{max} (°)	2.3, 31.3
Miller indices	-25 ≤ h ≤ 25, -13 ≤ k ≤ 13, -13 ≤ l ≤ 13
Measured reflections	10968
Independent reflections	2449
Reflections with *I* > 2σ (*I*)	2098
R_{int}	0.037
(sin θ/λ)$_{max}$ (Å^{-1})	0.732
Refinement	
$R[F^2 > 2s(F^2)]$, $wR(F^2)$, *S*	0.025, 0.055, 1.04
Number of variables	150
$\Delta\rho_{max}$, $\Delta\rho_{min}$ (e Å^{-3})	0.69, -0.81

Atomic positions and the corresponding displacement parameters are reported in table 2. Number of inter-atomic bond lengths are given in table 3 and geometrical features of hydrogen bond are listed in table 4. All representations were performed with Vesta-3 [26].

Structural description

In general, the structure of Hureaulite can be described as an open three-dimensional network of vertice-sharing octahedral-pentameric units with PO_4 and HPO_4 entities [27]. Similarly, the main building groups in the structure of $(Cd,Co)_5(HPO_4)_2(PO_4)_2.4H_2O$ are two conventional PO_4/HPO_4 tetrahedra and three $[(Cd(1)/Co(1))O_5(OH_2)]$, $[(Cd(2)/Co(2))O_6]$, and $[Co(3)O_4(OH_2)_2]$ octahedra of different distortion levels. This crystal structure can be described as five sequential octahedral $M_5^{II}O_{16}(OH_2)_6$ units of edge-sharing (Co(3)-Cd(1)/Co(1)-Cd(2)/Co(2)-Cd(1)/Co(1)-Co(3)) extending along the [100] direction (Figure 1). These units are interlinked by common vertices of $[(Cd(1)/Co(1))O_5(OH_2)]$, $[Cd(3)O_4(OH_2)_2]$, PO_4, and HPO_4 polyhedra in order to create a significant void parallel to the [001] direction. This interstitial space hosts the terminal H_2O molecules of the $[Co(3)O_4(OH_2)_2]$ groups (Figure 2), which interact with the neighboring oxygens by forming weak O—H---O hydrogen bonding. The O-H bond lengths and O-H..O bond angles reported for this compound are in line with those observed for some phosphates, viz. $SrFe(HPO_4)(PO_4)$ [15], $Co_2Pb(HPO_4)(PO_4)OH.H_2O$ [8], $AgMg_3(HPO_4)_2(PO_4)$ [13] and $Mg_{1.74}Cu_{1.26}(PO_4)_2.H_2O$ [28].

Table 2: Atomic coordinates and isotropic or equivalent thermal parameters (Å^2) in (Cd,Co)$_5$(HPO$_4$)$_2$(PO$_4$)$_2$.4H$_2$O.

Atom	Site	*x*	*y*	*z*	U_{iso}*/U_{eq}	Occ. (<1)
Cd1	8f	0.17512 (2)	1.02908 (3)	0.86715 (2)	0.01061 (8)	0.746 (3)
Co1	8f	0.17512 (2)	1.02908 (3)	0.86715 (2)	0.01061 (8)	0.254 (3)
Cd2	4e	0.000000	1.10659 (5)	1.250000	0.0105 (2)	0.340 (4)
Co2	4e	0.000000	1.10659 (5)	1.250000	0.0105 (2)	0.660 (4)
Co3	8f	0.31723 (2)	0.91445 (4)	0.68606 (4)	0.0099 (2)	
P1	8f	0.16150 (4)	0.73466 (8)	0.62584 (7)	0.0096 (2)	
P2	8f	0.08203 (4)	0.81870 (8)	1.09049 (7)	0.0102 (2)	
O1	8f	0.0770 (2)	0.7327 (2)	0.6568 (2)	0.0134 (4)	
O2	8f	0.1642 (2)	0.7532 (2)	0.4645 (2)	0.0149 (4)	
O3	8f	0.2013 (2)	0.5905 (2)	0.6741 (2)	0.0139 (4)	
O4	8f	0.2047 (2)	0.8636 (2)	0.7043 (2)	0.0147 (4)	
O5	8f	0.0839 (2)	0.8848 (2)	0.9426 (2)	0.0167 (4)	
O6	8f	0.0104 (2)	0.7142 (2)	1.0816 (2)	0.0183 (5)	
H6	8f	0.013984	0.650869	1.020986	0.027*	
O7	8f	0.1536 (2)	0.7274 (2)	1.1375 (2)	0.0165 (4)	
O8	8f	0.0753 (2)	0.9354 (2)	1.2021 (2)	0.0187 (5)	
O9	8f	0.2641 (2)	1.0817 (3)	0.5362 (2)	0.0158 (4)	
H9A	8f	0.245 (3)	1.147 (5)	0.587 (5)	0.04 (2)*	
H9B	8f	0.291 (3)	1.129 (5)	0.488 (5)	0.04 (2)*	
O10	8f	0.4196 (2)	1.0049 (3)	0.6569 (3)	0.0214 (5)	
H10A	8f	0.435 (3)	1.060 (7)	0.713 (7)	0.08 (2)*	
H10B	8f	0.455 (3)	0.959 (6)	0.645 (5)	0.05 (2)*	

Table 3: Chosen bond lengths in (Cd,Co)$_5$(HPO$_4$)$_2$(PO$_4$)$_2$.4H$_2$O.

Bond	Length (Å)	Bond	Length (Å)
Cd1/Co1—O2[a]	2.199 (2)	Co3—O4	2.058 (2)
Cd1/Co1—O8[b]	2.234 (2)	Co3—O3[c]	2.125 (2)
Cd1/Co1—O5	2.250 (2)	Co3—O7[f]	2.126 (2)
Cd1/Co1—O4	2.257 (2)	Co3—O2[g]	2.137 (2)
Cd1/Co1—O3[c]	2.320 (2)	< Co3—O> = 2.1138 Å	
Cd1/Co1—O9[a]	2.333 (2)	P1—O3	1.528 (2)
< Cd1/Co1—O> = 2.2655 Å		P1—O4	1.539 (2)
Cd2/Co2—O8	2.124 (2)	P1—O2	1.546 (2)
Cd2/Co2—O8[e]	2.124 (2)	P1—O1	1.546 (2)
Cd2/Co2—O5[a]	2.212 (2)	< P1—O> = 1.5396 Å	
Cd2/Co2—O5[d]	2.212 (2)	P2—O8	1.512 (2)
Cd2/Co2—O1[a]	2.240 (2)	P2—O7	1.529 (2)
Cd2/Co2—O1[d]	2.240 (2)	P2—O5	1.530 (2)
< Cd2/Co2—O> = 2.1921 Å		P2—O6	1.571 (2)
Co3—O10	2.025 (3)	< P2—O> = 1.5353 Å	
Co3—O9	2.211 (2)		

Note: Symmetry indicators: (a) x, -y+2, z+1/2; (b) x, -y+2, z-1/2; (c) -x+1/2, y+1/2, -z+3/2; (d) -x, -y+2, -z+2; (e) -x, y, -z+5/2; (f) -x+1/2, -y+3/2, -z+2; (g) -x+1/2, -y+3/2, -z+1; and (h) -x+1/2, y-1/2, -z+3/2.

Table 4: Hydrogen-bond geometry (Å, °) in (Cd,Co)$_5$(HPO$_4$)$_2$(PO$_4$)$_2$.4H$_2$O.

D—H···*A* (°)	*D*—H (Å)	H···*A* (Å)	*D*···*A* (Å)	*D*—H···*A* (°)
O6—H6···O10[c]	0.82	2.53	3.299 (3)	156
O9—H9*A*···O7[a]	0.86 (5)	2.07 (5)	2.850 (3)	151 (4)
O9—H9*B*···O7[b]	0.82 (5)	1.85 (5)	2.666 (3)	174 (5)
O10—H10*A*···O1[b]	0.76 (7)	2.02 (7)	2.715 (3)	153 (6)
O10—H10*B*···O6[d]	0.77 (5)	1.98 (5)	2.696 (3)	155 (5)

Note: Symmetry indicators: (a) x, -y+2, z-1/2; (b) -x+1/2, y+1/2, -z+3/2; (c) -x+1/2, y-1/2, -z+3/2; and (d) x+1/2, -y+3/2, z-1/2.

Table 5: BVS and CD analysis in (Cd,Co)$_5$(HPO$_4$)$_2$(PO$_4$)$_2$.4H$_2$O.

Ion	C(j).SO(j)	CN(j)	ECoN(j)	BVS(j)	Q(j)	C(j)/Q(j)
Co(1)/Co(1)	2	6	5.91	1.98	1.88	1.07
Cd(2)/Co(2)	2	6	5.89	1.84	1.82	1.10
Co(3)	2	6	5.83	1.68	1.98	1.01
P(1)	5	4	4.00	4.93	5.24	0.95
P(2)	5	4	3.97	5.00	4.70	1.06
H6	1	1	1.00	1.16	0.94	1.06
H9A	1	1	1.19	1.08	0.86	1.16
H9B	1	1	1.28	1.15	0.87	1.14
H10A	1	1	1.13	1.03	0.86	1.17
H10B	1	1	1.10	1.03	0.85	1.17

Note: C(j) = oxidation state; SO(j) = site occupancy factor; CN(j) = coordination number; Q(j) = computed charge; BVS(j) = computed valence; and ECoN(j) = effective coordination number.

Analysis of the structural model

In this paper, the BVS and CD analysis tools were used to evaluate the reliability and stability of the given structural model of (Cd,Co)$_5$(HPO$_4$)$_2$(PO$_4$)$_2$.4H$_2$O. The ionic charge repartitions and the BVS results were provided by the CHARDI-2015 [29] and EXPO-2014 programs [30], respectively (Table 5).

In this structure, all atoms occupy the general positions 8f of the C2/c space group (No. 15), excluding (Cd2/Co2), that are located at a particular position 4e on a 2-fold rotation axis. According to the distribution of cationic charges over 10/20 distinct crystallographic positions, (Cd^{2+}/Co^{2+}), Co^{2+}, P^{5+}, and H^+ entirely fill their corresponding sites. To ensure charge balance, the oxygen atoms are arranged in the remainder of positions. All computed charges $Q(j)_{cations}$ are in complete conformity with their corresponding weighted oxidation numbers Q(j).SO(j). Also their charge ratios $(C(j)/Q(j))_{cations} \approx 1$ which proves the accuracy of this repartition scheme. This result is also supported by the lower deviation of Q(j) from C(j) which is corroborated by the absolute mean (MAPD) of 8.8%. By carefully analyzing the calculated cationic BVS(j) against their theoretical valences V(j), the BVS approach also leads to the predicted values with a good overall instability index (GII = 0.080 v.u). In this structure, the first positive site is completely filled by the cobalt Co^{2+}(3) while (Cd^{2+}(1)/Co^{2+}(1)), (Cd^{2+}(2)/Co^{2+}(2)) cations occupy each other's two mixed sites with the respective occupancy rates of 0.2/0.5 and 09/05. These sites are tightly bounded with six surrounding oxygen atoms, producing more or less distorted octahedra with a considerable tractive stress. This fact is supported by bonds valences BVS(M) < V(M) [31] and the distortion index (bond length) values ($BLD = \frac{\sum_{i=1}^{6}|(M-O)_i - \langle M-O \rangle|}{6\langle M-O \rangle}$ where M = Co^{2+} or Cd^{2+}/Co^{2+}) $BLD_{Cd(1)/Co(1)}$ = 0.01793, $BLD_{Cd(2)/Co(2)}$ = 0.02071 and $BLD_{Co(3)}$ = 0.02275 [32]. According to the coordination values of ECoN (Pi)/CN(Pi) (I = 1 or 2), both P atoms are arranged in a typical tetrahedral geometry. The last crystallographic sites are filled by H6, H9A, H9B, H10A, and H10B cations which form weak hydrogen bonds with suitable coordination of ECoN(H6) = 1.00, ECoN(H9A) = 1.19, ECoN(H9B) = 1.28, ECoN(H10A) = 1.13, and ECoN(H10B) = 1.10 [33].

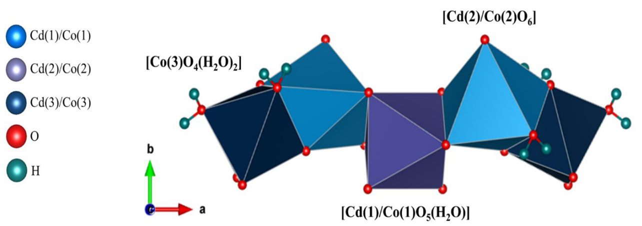

Figure 1: Edge-sharing [(Cd(1)/Co(1))O$_5$(OH$_2$)], [(Cd(2)/Co(2))O$_6$], and [Co(3)O$_4$(OH$_2$)$_2$] arrangement parallel to the [100].

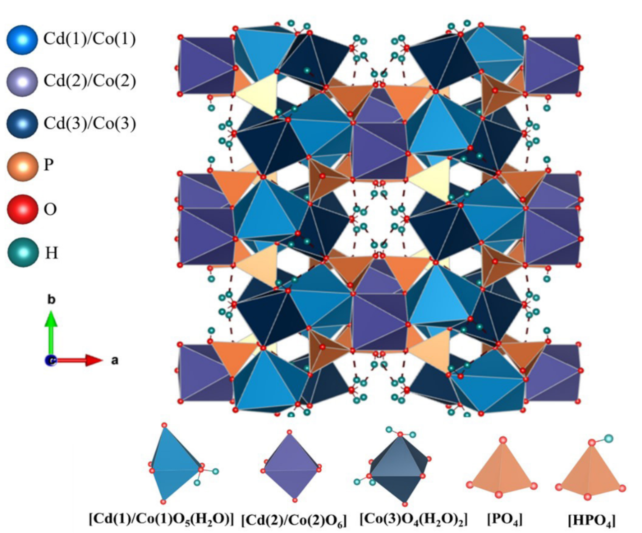

Figure 2: Perspective view of (Cd,Co)$_5$(HPO$_4$)$_2$(PO$_4$)$_2$.4H$_2$O crystal structure along the c-axis revealing hydrogen bonding (dashed lines).

Conclusion

Single crystals of the novel phosphate (Cd,Co)$_5$(HPO$_4$)$_2$(PO$_4$)$_2$.4H$_2$O, belonging to the Hureaulite family, were synthesized by the hydrothermal process and studied by single crystal X-ray diffraction. The adequacy of the resulting structural model was confirmed by BVS and CD analyses. This net-framework is made up of sequential octahedral $M_5^{II}O_{16}(OH_2)_6$ edge-sharing units (M^{II} = Co or Cd/Co) running along the [100] direction. These units are joined by common vertices of [(Cd(1)/Co(1))O$_5$(OH$_2$)], [(Cd(3)O$_4$(OH$_2$)$_2$], PO$_4$, and HPO$_4$ polyhedra to generate a sizeable cavities parallel to the [001] direction. This interstitial space contains the terminal H_2O molecules of the [Co(3) O$_4$(OH$_2$)$_2$] groups, that react with adjacent oxygen atoms by forming a weak O-H--O hydrogen bonding.

Acknowledgements

The authors are very grateful to the UATRS-CNRST, Rabat, Morocco for the X-ray analysis.

Conflict of Interest

None.

Funding

The current work was entirely funded by Mohammed V University, Rabat, Morocco.

References

1. Rao CNR, Natarajan S, Neeraj S. 2000. Building open-framework metal phosphates from amine phosphates and a monomeric four-membered ring phosphate. *J Solid State Chem* 152(1): 302-321. https://doi.org/10.1006/jssc.2000.8676
2. Colomban P. 1992. Proton Conductors: Solids, Membranes and Gels - Materials and Devices. Cambridge University Press.
3. Patil SS, Shin JC, Patil PS. 2022. Binder free hydrothermally synthesized nickel phosphate hydrate microplates on nickel foam for supercapacitors. *Ceram Int* 48(19): 29484-29492. https://doi.org/10.1016/j.ceramint.2022.07.050
4. Westberg HJ, Nilsson PH, Rosén BG, Stenbom B. 2000. Manganese phosphating of gears and surface roughness consequence. *Tribol Ser* 38: 145-153. https://doi.org/10.1016/S0167-8922(00)80120-0
5. Arcibar-Orozco JA, Avalos-Borja M, Rangel-Mendez JR. 2012. Effect of phosphate on the particle size of ferric oxyhydroxides anchored onto activated carbon: As(V) removal from water. *Environ Sci Technol* 46(17): 9577-9583. https://doi.org/10.1021/es204696u
6. Frost RL, Xi Y, Scholz R, López A, Belotti FM. 2013. Vibrational spectroscopic characterization of the phosphate mineral hureaulite–(Mn, Fe)$_5$(PO$_4$)$_2$(HPO$_4$)$_2$.4(H$_2$O). *Vibr Spectrosc* 66: 69-75. https://doi.org/10.1016/j.vibspec.2013.02.003
7. Assani A, Saadi M, Zriouil M, El Ammari L. 2011. Heptamagnesium bis(phosphate) tetrakis(hydrogen phosphate) with strong hydrogen bonds: Mg$_7$(PO$_4$)$_2$(HPO$_4$)$_4$. *Acta Cryst Sec E Cryst Commun* 67(10): i52. https://doi.org/10.1107/S1600536811036361
8. Assani A, Saadi M, Zriouil M, El Ammari L. 2012. Dicobalt(II) lead(II) hydrogenphosphate(V) phosphate(V) hydroxide monohydrate. *Acta Cryst Sec E Cryst Commun* 68(5): i30. https://doi.org/10.1107/S1600536812014870

9. Assani A, Saadi M, Zriouil M, El Ammari L. 2012. Dilead(II) trimanganese(II) bis(hydrogenphosphate) bis(phosphate). *Acta Cryst Sec E Cryst Commun* 68(8): i66. https://doi.org/10.1107/S1600536812033259

10. Khmiyas J, Assani A, Saadi M, El Ammari L. 2013. Distrontium trimanganese(II) bis(hydrogenphosphate) bis(orthophosphate). *Acta Cryst Sec E Cryst Commun* 69(8): i50. https://doi.org/10.1107/S1600536813018898

11. Assani A, El Ammari L, Zriouil M, Saadi M. 2011. Disilver(I) tricobalt(II) hydrogenphosphate bis(phosphate), $Ag_2Co_3(HPO_4)(PO_4)_2$. *Acta Cryst Sec E Cryst Commun* 67(7): i41. https://doi.org/10.1107/S1600536811022598

12. Assani A, El Ammari L, Zriouil M, Saadi M. 2011. Disilver(I) trinickel(II) hydrogenphosphate bis(phosphate), $Ag_2Ni_3(HPO_4)(PO_4)_2$. *Acta Cryst Sec E Cryst Commun* 67(7): i40. https://doi.org/10.1107/S1600536811021167

13. Assani A, Saadi M, Zriouil M, El Ammari L. 2011. Silver trimagnesium phosphate bis(hydrogenphosphate), $AgMg_3(PO_4)(HPO_4)_2$, with an alluaudite-like structure. *Acta Cryst Sec E Cryst Commun* 67(1): i5. https://doi.org/10.1107/S1600536810053304

14. Khmiyas J, Benhsina E, Ouaatta S, Assani A, Saadi M, et al. 2020. Crystal structure of silver strontium copper orthophosphate, $AgSr_4Cu_{4.5}(PO_4)_6$. *Acta Cryst Sec E Cryst Commun* 76(2): 186-191. https://doi.org/10.1107/S2056989020000109

15. Khmiyas J, Assani A, Saadi M, El Ammari L. 2022. Crystal structure, charge-distribution and bond-valence-sum investigations of a new layered phosphate $SrFe(HPO_4)(PO_4)$. *Mater Today Proc* 58: 994-998. https://doi.org/10.1016/j.matpr.2021.12.458

16. Alluaud F. 1826. Notices sur l'hétérosite, l'hureaulite (fer et manganèse phosphatés), et sur quelques autres minéraux du département de la Haute-Vienne. *Ann Sci Nat* 8: 334-354.

17. Dufrénoy A. 1829. Sur deux nouveaux phosphate de manganese et fer. *Ann Chem Phys* 41: 337-345.

18. Moore PB, Araki T. 1973. Hureaulite, $Mn_5^{2+}(H_2O)_4[PO_3(OH)]_2[PO]_4]_2$: its atomic arrangement. *Am Miner* 58(3-4): 302-307.

19. Altermatt D, Brown ID. 1985. The automatic searching for chemical bonds in inorganic crystal structures. *Acta Cryst Sec B Struct Sci Cryst Eng Mater* 41(4): 240-244. https://doi.org/10.1107/S0108768185002051

20. Nespolo M. 2016. Charge distribution as a tool to investigate structural details. IV. A new route to heteroligand polyhedra. *Acta Cryst Sec B Struct Sci Cryst Eng Mater* 72(1): 51-66. https://doi.org/10.1107/S2052520615019472

21. Bruker SAINT-Plus. 2012. Bruker AXS Inc., Madison, Wisconsin, USA.

22. Krause L, Herbst-Irmer R, Sheldrick GM, Stalke D. 2015. Comparison of silver and molybdenum microfocus X-ray sources for single-crystal structure determination. *J Appl Cryst* 48(1): 3-10. https://doi.org/10.1107/S1600576714022985

23. Farrugia LJ. 2012. WinGX and ORTEP for Windows: an update. *J Appl Cryst* 45(4): 849-854. https://doi.org/10.1107/S0021889812029111

24. Sheldrick GM. 2015. SHELXT-Integrated space-group and crystal-structure determination. *Acta Cryst Sec A Found Adv* 71(1): 3-8. https://doi.org/10.1107/S2053273314026370

25. Sheldrick GM. 2015. Crystal structure refinement with SHELXL. *Acta Cryst Sec C Struct Chem* 71(1): 3-8. https://doi.org/10.1107/S2053229614024218

26. Momma K, Izumi F. 2011. VESTA 3 for three-dimensional visualization of crystal, volumetric and morphology data. *J Appl Cryst* 44(6): 1272-1276. https://doi.org/10.1107/S0021889811038970

27. Hartl A, Jurányi F, Krack M, Lunkenheimer P, Schulz A, et al. 2022. Dynamically disordered hydrogen bonds in the hureaulite-type phosphatic oxyhydroxide $Mn_5[(PO_4)_2(PO_3(OH))_2](HOH)_4$. *J Chem Phys* 156(9): 094502. https://doi.org/10.1063/5.0083856 +

28. Khmiyas J, Assani A, Saadi M, El Ammari L. 2022. Elaboration and characterization of a new phosphate $Mg_{1.74}Cu_{1.26}(PO_4)_2.H_2O$ with morphotropic structure. *Mater Today Proc* 58: 1069-1073. https://doi.org/10.1016/j.matpr.2022.01.126

29. Nespolo M, Guillot B. 2016. CHARDI2015: charge distribution analysis of non-molecular structures. *J Appl Cryst* 49(1): 317-321. https://doi.org/10.1107/S1600576715024814

30. Altomare A, Cuocci C, Giacovazzo C, Moliterni A, Rizzi R, et al. 2013. EXPO2013: a kit of tools for phasing crystal structures from powder data. *J Appl Cryst* 46(4): 1231-1235. https://doi.org/10.1107/S0021889813013113

31. Yamada I, Takamatsu A, Ikeno H. 2018. Complementary evaluation of structure stability of perovskite oxides using bond-valence and density-functional-theory calculations. *Sci Technol Adv Mater* 19(1): 101-107. https://doi.org/10.1080/14686996.2018.1430449

32. Redhammer GJ, Roth G, Tippelt G, Bernroider M, Lottermoser W, et al. 2004. The mixed-valence iron compound $Na_{0.1}Fe_7(PO_4)_6$: crystal structure and ^{57}Fe Mössbauer spectroscopy between 80 and 295 K. *J Solid State Chem* 177(4-5): 1607-1618. https://doi.org/10.1016/j.jssc.2003.12.016

33. Nespolo M, Ferraris G, Ivaldi G, Hoppe R. 2001. Charge distribution as a tool to investigate structural details. II. Extension to hydrogen bonds, distorted and hetero-ligand polyhedra. *Acta Cryst Sec B Struct Sci* 57(5): 652-664. https://doi.org/10.1107/S0108768101009879